THE IMPACT OF RANDOM DEBRIS ON THE PERFORMANCE OF SINGLE SATELLITE AND CONSTELLATIONS

Yuyan LIU(1), Baojun Pang(1), Diqi HU(1), Runqiang CHI(1), wuxiong CAO(1), Wen SUN(1), Xuan CHU(1)

(1)Hypervelocity Impact Research Center, Harbin Institute of Technology, Harbin (China), Email: liuyy@stu.hit.edu.cn

ABSTRACT

Space debris, particularly undetectable hazardous debris, presents significant uncertainties for spacecraft, including potential component failures, and even overall mission unsuccess. To address this issue, this paper proposes an algorithm to assess the uncertain impact of debris impacts on satellites and constellations. Satellite geometric models, functional failure model, and debris distribution are incorporated into the algorithm to establish a mapping between the number of debris impacts and the failure probability of satellite. Based on this, the paper discusses the impact of the position and number of failed satellites within the constellation on coverage performance. The results indicate that if the positions of failed satellites are randomly distributed, the change in coverage performance is minimal. As the number of failed satellites increases, the rate of decline in coverage performance accelerates. This algorithm links debris to constellation performance, enabling predictions based on impact counts, aiding spacecraft protection and constellation optimization.

1 INTRODUCTION

In recent years, the frequency of space launches has increased significantly. In 2023 alone, nearly 3,000 spacecrafts were successfully placed into orbit, accounting for nearly one-fifth of the cumulative number launched prior to that year [1]. At the same time, the amount of space debris is increasing, posing a great threat to the safe operation of spacecraft [2][3]. This is especially true for large constellations, where satellite disintegration events can greatly increase the debris density in the surrounding environment, potentially leading to the failure of nearby satellites. Due to the inability to detect small debris, the impacts have uncertainties, including the location and the number of impacts, leading to differences in the final state of the satellites, which in turn affects the performance of the constellations and mission fulfillment. Therefore, the uncertainty of debris impacts is a key factor in the design of satellite and constellations.

Regarding the impact of debris impact on the performance of single satellites, various institutions have developed software using failure probability as an evaluation metric. Methodologically, BUMPER [4] and ESABASE [5] can further calculate the diameter and depth of impact craters based on survivability assessments. Hu [6] proposed a ray method based on virtual outer walls to analyze spacecraft susceptibility. While balancing computational efficiency and accuracy, Chi [7] further calculated the optimal matching relationship between the parameters of the virtual outer wall and the geometric model of the spacecraft. Lorenzo [8] analyzed the potential damage caused by secondary debris on satellite subsystems. Despite ongoing efforts by scholars to refine their methods, the structural complexity of single satellites is often neglected. Traditional fault tree analysis, when confronted with the uncertainties of debris impacts—such as random impact directions and locations that lead to diverse component damages, fails to comprehensively enumerate all possible failure scenarios.

When conducting vulnerability assessments, that is, analyzing the damage to components under foregone impact, the structural failure of components is generally equated with functional failure. Wilmer [9] evaluated the vulnerability of a component based on the Ballistic Limit Equation (BLE). Trisolini [10] and others improved the BLE method by combining the debris cloud model (DCM), which more realistically reflects the damage caused by secondary debris to the interior of the spacecraft. However, both methods essentially evaluate failure based on whether the component is penetrated or not. But even if small debris does not penetrate the component, it still causes a certain degree of damage to the component. As the number of impacts increases, the component may undergo functional degradation or even failure. Therefore, previous vulnerability assessment methods for components are unable to characterize this quantitatively cumulative impact.

Regarding the assessment of the impact of debris impacts on constellations, Pardini [11] analyzed the impact of disintegrating debris from Cosmos 1408 on the Starlink constellation. Polli [12] proposed a model for calculating the collision probability between deorbiting or launching spacecraft and constellations. Tao [13] analyzed the probability of secondary collision between the debris cloud generated by a collision within the Starlink constellation and satellites in the same orbit. Yuan [14] used the continuum approach to assess the impact of satellite explosions on the total number of space objects in the orbital layer of constellation. Sun[15] analyzed the coverage performance of the constellation based on the Markov-ADC model, but did not consider that the distribution of failed satellites might have different impacts on the constellation system. Wen[16] analyzed the

Proc. 9th European Conference on Space Debris, Bonn, Germany, 1–4 April 2025, published by the ESA Space Debris Office
Editors: S. Lemmens, T. Flohrer & F. Schmitz, (http://conference.sdo.esoc.esa.int, April 2025)

variation of constellation availability for navigation constellations with different numbers of satellite failures. In summary, current research on the impact of debris on constellations, focuses on impact probability calculations, but fails to quantify the impacts on constellation performance; on the other hand, it tends to analyze the performance after satellite failures within the constellation, only considering the failure probabilities arising from the own reliability of satellites. There is no coherent analytical link formed between debris impacts and constellation performance.

The uncertainty of debris impact is mainly reflected in the unknown characteristics of debris data, i.e., impact direction and location. This paper proposes an algorithm to assess the impact of debris impact uncertainty on the satellite and the constellation, which can be divided into two parts: the risk assessment of a single satellite and the performance assessment of the constellation. The assessment process is shown in Fig. 1.

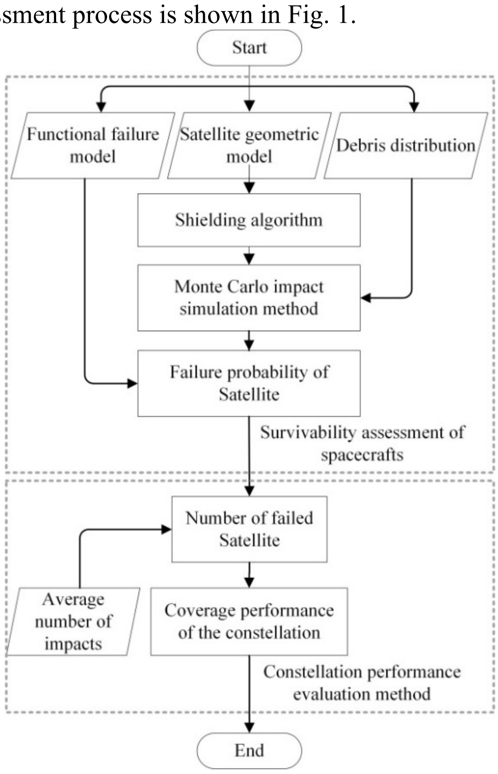

Figure 1 Assessment process of the impact of debris on constellation performance

For the risk assessment of a single satellite, this paper takes the satellite geometry model, functional failure model, and debris distribution as inputs. Based on the shielding algorithm and Monte Carlo impact simulation method, the correspondence between the number of impacts and the probability of satellite failure is obtained. In the assessment of constellation performance impact, the expectation of the number of failed satellites is obtained by combining the average number of impacts on the satellites in the constellation. Finally, the impacts of the location and number of failed satellites on the coverage performance of the constellation are analyzed.

2 RISK ASSESSMENT OF DEBRIS IMPACTS ON SINGLE SATELLITE

This section presents a risk assessment method for single satellite based on shielding algorithm and Monte Carlo impact simulation. First, the geometric model of the spacecraft is analyzed using the shielding algorithm to determine the shielding relationships among components under different impact directions. Second, based on the impact direction, the impact position is selected using Monte Carlo method, and combined with the spacecraft failure model to determine whether the components fail, thereby assessing whether the spacecraft fails. Finally, the failure probability of the spacecraft under different numbers of impacts is determined by combining the multiple impact simulations.

2.1 Calculation of Exposed Elements Based on Shielding Algorithm

In the event of a debris impact on a spacecraft, the components in front will shield those behind, preventing them from being hit. The shielding relationship among spacecraft components will lead to different probabilities of impact for different components, meaning that the susceptibility of the components varies. To quantify the difference in susceptibility between components caused by the uncertainty in the direction of debris impact, it is necessary to analyze the component exposure based on a geometric model of the spacecraft. As shown in Fig. 2, in the incoming direction of space debris, component A behind the protective structure is shielded by component B. The projected area of component A shielded in the incoming direction is called the shielded area of component A, denoted as S_s, and the projected area of component A exposed to the incoming direction of space debris is called the exposed area of component A, denoted as S_e.

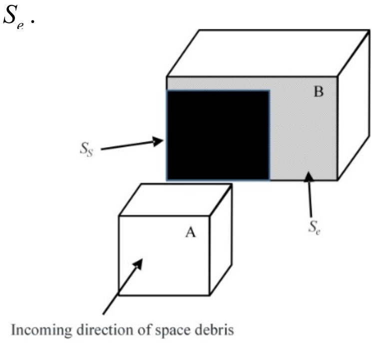

Figure 2 Schematic diagram of component shielding relationship

The exposure coefficient of component A is given by:

$$\eta_a = S_e / (S_e + S_s) \tag{1}$$

Let the finite element set of component A be E_A, as expressed as:

$$E_A = \{a_j \in E | j = 1, 2 \cdots N_A\} \tag{2}$$

Since the area of the finite element is small, for a certain finite element a_j, it can be assumed that it has only two states: completely occluded and completely exposed. Thus, the finite element set of component A can be divided into the set of exposed finite elements E_e and the set of occluded finite elements E_s, we have:

$$E_e = \{a_j | \eta_{a_j} = 1\} \tag{3}$$

$$E_s = \{a_i | \eta_{a_i} = 0\} \tag{4}$$

The exposed area of the component A is given by:

$$S_e = \sum_{i=1}^{N_A} \{S_{a_i} | a_i \in E_e\} \tag{5}$$

The exposure coefficient of the component A is:

$$\eta_a = \frac{\sum \{S_{a_j} | a_j \in E_e\}}{\sum \{S_{a_i} | a_i \in E_s\}} \tag{6}$$

2.2 Impact Simulation Based on Monte Carlo Method

Spacecraft risk assessment in the space debris environment considers the impact of space debris on spacecraft as a source of risk. This involves a quantitative analysis of the probability of space debris impact and spacecraft failure [17]. Given the uncertainty of the debris impact location, this paper employs Monte Carlo method to select the impact location based on the debris distribution. It assumes the failure of the impacted element, conducts multiple impact simulations until spacecraft failure, and repeats the simulation in multiple directions. This approach is used to determine the relationship between the failure probability of the spacecraft and the number of impacts.

To ensure the uniformity of the input when the functional failure model of the spacecraft components/systems is given, Eq. (6) is adopted to simplify the characterization of the failure probability of the components/systems.

$$P = \begin{cases} 0, & n < n_1 \\ \dfrac{n - n_1}{n_2 - n_1}, & n_1 \le n < n_2 \\ 1, & n \ge n_2 \end{cases} \tag{7}$$

Where n_1 is the minimum number of failure elements for the component or the minimum number of failed components of the same type, and n_2 is the number of complete failure elements for the component or the number of failed components of the same type when the system fails, and P the failure probability of the component/system. This paper assumes that if any type of component reaches the system failure condition, the system fails.

Due to the fact that debris striking a spacecraft can also cause the surrounding elements to fail, a ratio of affected area to penetration area is used to more realistically describe this phenomenon, that is, the ratio of the total area of failure elements to the area of the penetration [18], as shown in Fig. 3.

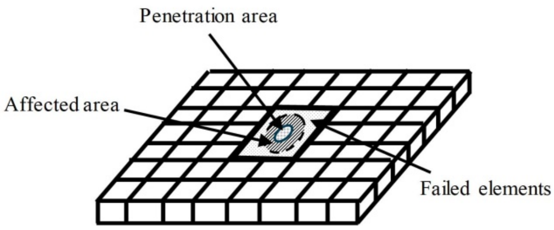

Figure 3 Schematic diagram of the impact range ratio

The traditional approach of risk assessment generally starts from the debris flux in the orbit of the spacecraft, analyzing its failure risk in orbit in conjunction with material and component layout of the spacecraft. This paper focuses on the problems caused by the uncertainty of debris impact, and simplifies the complex impact situation into the number of failure elements, and then calculates the failure probability of the spacecraft. In this way, the cumulative effect of debris impacts on spacecraft damage can be clearly described, and on the other hand, the problem of too many failure scenarios generated by the uncertainty of debris impacts, which cannot be enumerated by the traditional fault tree method, is also solved. The flow of the spacecraft risk assessment method based on Monte Carlo method impact simulation is shown in Algorithm 1. It is assumed that a single impact must lead to the failure of the first two layers of the impacted elements in that direction, and the analysis can be carried out by combining the number of debris corresponding to the critical size of the component impact in practical applications.

Algorithm 1

1. **Input:** $M_G, M_F, M_D, R, N_{dir}, N_{\exp}$
2. $i = 1$, where i denotes the index of the debris flow direction in the coordinate system
3. **While** the number of debris flow directions $N_{dir} \ge i$ **do**
4. $j = 1$, j where j represents the number of impact simulations already performed for the direction

5. **While** the number of debris flow directions $N_{\exp} \geq j$ **do**

6. Calculate the exposed element indices N_e of the satellite geometric model M_G using the occlusion algorithm.

7. Compute the projected area A_p of the satellite in the given direction

8. $k = 1$, where k represents the number of impacts already performed in the current simulation

9. Select the impacted element index N_j based on Monte Carlo method, and determine the component index U to which the element belongs.

10. Calculate the collateral failure elements N_{ass} based on the impact range ratio, and compute the total number of failed facets n

11. **if** $n < n_1$ **then**

12. Component failure probability $P = 0$, $k = k + 1$

13. **Else if** $n_1 < n < n_2$ **then**

14. $P = (n - n_1)/(n_2 - n_1)$, generate a random number Ran

15. **If** $Ran > P$ **then**

If the system fails

16. **Output:** $\left[k, n, \sum N_j, \sum N_{ass},\right]$

Else

$k = k + 1$

end

17. **Else**

18. $k = k + 1$

19. **End**

20. **Else**

If the system fails

21. **Output:** $\left[k, n, \sum N_j, \sum N_{ass},\right]$

Else

$k = k + 1$

end

22. **End**

23. $j = j + 1$

24. **End**

25. $i = i + 1$

26. **End**

Accumulate the total number of impacts k for all impact simulations

Compute the ratio of impact counts to the total number of simulations

Obtain the single-satellite failure probability density distribution

Establish the relationship between impact counts and single satellite failure probability

Where M_G is the geometrical model of the satellite; M_F is the failure model of the satellite, including the serial numbers of the satellite components and the maximum and minimum number of failed units; M_D is the size of the debris; R is the ratio of the influence areas; N_{Dr} is the number of debris incoming directions; $N_{\exp}$ is the number of simulations in a single direction.

2.3 Simulation of single satellite

The satellites are mostly composed of a combination of truss and box-panel structures [17]. A single-satellite geometric model in Fig. 4 is analyzed as an example, which features a truss as the main framework structure, with instruments mounted on the side panels and the propulsion components installed on the base plate.

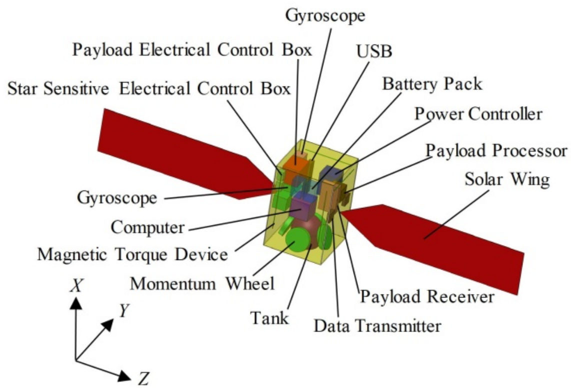

Figure 4 Truss and box-panel structure combination platform

This satellite consists of 27 components, and the functional failure models of each component are shown in Table 1

.

Table 2 Component functional failure models

Component number	Component name	Component n_1	Component n_2	Component type Number	System $n_1 = n_2$
1	Solar wing	25	265	1	1
2	Solar wing	25	265	1	

3	Storage box	1	6	2	1
4	Momentum wheel	1	6	3	
⋮	⋮	⋮	⋮	⋮	2
7	Momentum wheel	1	6	3	
8	Gyroscope	1	6	4	
⋮	⋮	⋮	⋮	⋮	1
10	Gyroscope	1	6	4	
11	Magnetic Moment Device	1	6	5	
⋮	⋮	⋮	⋮	⋮	1
14	Magnetic Moment Device	1	6	5	
15	USB	1	6	6	2
16	USB	1	6	6	
17	Star Sensor	1	6	7	2
18	Star Sensor	1	6	7	
19	battery	1	6	8	2
20	battery	1	6	8	
21	Data Transmission Transmitter	1	6	9	2
22	Data Transmission Transmitter	1	6	9	
23	Power Control Box	1	6	10	1
24	Payload	1	6	11	1
25	Payload	1	6	11	
26	Skin	0	960	12	1
27	Computer	1	4	13	1

The correspondence between the number of debris impacts and the spacecraft failure probability density distribution after 3080 simulations is shown in Fig. 5 The minimum number of impacts is 1, as the debris directly penetrated the outer shell and hit the key internal components. The maximum value is 83, with the impact locations primarily concentrated on the solar panels. The peak number of impacts occurs between 10 and 20, with the cumulative number of simulations in this range accounting for approximately 42% of the total simulations, indicating that half of the spacecraft will fail after more than ten impacts. Even if the spacecraft does not completely lose its operational capability, the potential for collateral effects from debris impacts on critical components, such as cables, may significantly degrade the actual performance of the spacecraft.

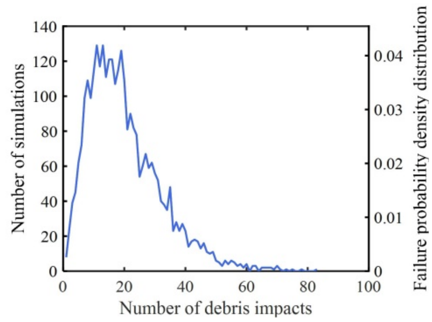

Figure 5 Correspondence between impact count and impact simulation count

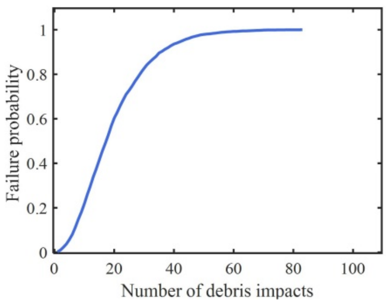

(a) One direction impact

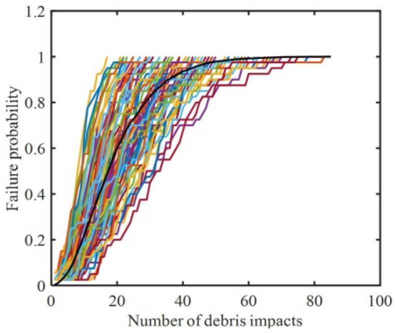

(b) All direction impact

Figure 6 Failure probability of the spacecraft under different impact counts

Fig. 6 shows the failure probability of the spacecraft under different numbers of impacts and Fig. 6(a) depicts the failure probability when the debris impacts from only one direction, while Fig. 6(b) covers the results of impacts in all directions, calculated from the cumulative impact number shown in Fig. 5. It can be seen that the failure probability reaches 80% when the number of impacts in that direction reaches about 30. By overlaying the failure probability graphs from various directions, as shown in the right image, it is evident that when the impact count is 20, the failure probability in some directions has already reached 100%, while in others it is only 20%. This indicates that the uncertainty of debris impact direction and location has a significant impact on the survivability of spacecraft.

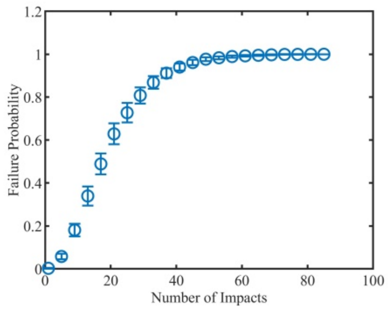

Figure 7 Failure Probability of the Spacecraft at Confidence Level 0.95

Fig. 7 shows the variation of failure probability of the Spacecraft with the number of impacts at a confidence level of 0.95. Combining the data in all directions, the probability of spacecraft failure reaches 80% after about 30 impacts and nearly 100% after more than 50 impacts.

3 ASSESSMENT OF THE UNCERTAINTY DEBRIS IMPACT ON CONSTELLATION PERFORMANCE

In this section, the number of failed satellites in the constellation is calculated based on data on the number of impacts on spacecraft in the constellation, and the impact of differences in the location and number of failed satellites in the constellation on coverage performance is discussed.

3.1 Calculation of the Number of Failed Spacecraft

The correspondence between the failure probability of a spacecraft and the number of impacts can be obtained from the previous section, and then the average failure probability of a spacecraft at the number of impacts can be obtained, denoted as P. If the maximum number of spacecraft impacts in the constellation is t, and the number of spacecraft with i impacts is N_i, where $(i = 0,1,2\cdots,t)$, the failure probability of spacecraft with this number of impacts is P_i, then the expected number of failed spacecraft is N:

$$N = N_i \times P_i \tag{8}$$

Thus, the total number of failed spacecrafts in the constellation is N_t:

$$N_t = \sum_{i=0}^{t} N \tag{9}$$

3.2 Entropy Weight Method

Due to the different focuses of different coverage indicators, the weights of different indicators need to be adjusted. The methods for determining weights are mainly divided into subjective weighting methods and objective weighting methods. Among them, subjective weighting methods are greatly influenced by the subjective intentions of experts, while the entropy weight method in objective weighting methods determines the weights based on the amount of information contained in each indicator [20]. This paper will use the entropy weight method to determine the weight of each indicator.

Due to the different attributes of each indicator, it is necessary to normalize the raw data. The indicator parameters are subdivided into positive and inverse indicators, where the values of positive indicators are consistent with performance levels, while the values of negative indicators are inversely related to performance levels. If there are l objects and m evaluation indicators, the raw data matrix is

$X = [x_{ij}]_{l\times m}, x_{ij} \geq 0 (i = 1,2,\cdots,l; j = 1,2,\cdots,m)$.

The normalization is performed for both positive and negative indicators[20]:

$$x'_{ij\text{pos}} = \frac{x_{ij} - x_{j\min}}{x_{j\max} - x_{j\min}}, x'_{ij\text{neg}} = \frac{x_{j\max} - x_{ij}}{x_{j\max} - x_{j\min}} \quad (10)$$

$$p_{ij} = x'_{ij} / \sum_{i=1}^{l} x'_{ij} \quad (11)$$

The normalized matrix is $P = [p_{ij}]_{l\times m}$.

For a certain indicator x_j in the system, its information entropy is[20]:

$$E_j = -k \sum_{i=1}^{l} (p_{ij} \ln p_{ij}) \quad (12)$$

where $k = 1/\ln l$.

The entropy weight ω_j of the j th indicator is defined as [20]:

$$\omega_j = \frac{1 - E_j}{m - \sum_{j=1}^{m} E_j} \quad (13)$$

3.3 Simulation of Constellation performance

Taking Walker constellation as the analysis object, this constellation is divided into two orbital layers, with orbital altitudes of 550 km and 540 km respectively. Each altitude layer has 22 orbital planes, with each plane containing 72 satellites, totaling 3,168 satellites. All orbital configurations employ an inclination of 53°. The on-board sensor is a simple cone sensor with a cone angle of 45°. The coverage area is set to be within [73°33'E, 135°05'E], and [3°51'N, 53°33'N].

Assuming that each spacecraft in the constellation experiences an average of 29 impacts and follows a Poisson distribution, the number of impacts by space debris is shown in Fig. 8. Combining the simulation results from Section 2.3, it can be derived from equations (7) and (8) that the expected number of failed spacecrafts in the constellation is 638, accounting for approximately 20% of the total number of satellites.

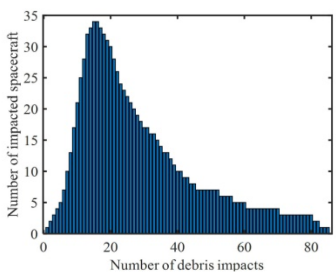

Figure 8 Correspondence between the number of impacts on satellites and impacted spacecraft quantity

Considering that the uncertainty of debris can affect the position distribution of failed satellites, this paper analyzes the impact of the position of failed satellites on the constellation coverage performance by integrating three indicators: coverage duration, coverage multiplicity, and maximum revisiting time with the entropy weight method. Additionally, considering that Kessler Syndrome may lead to a higher number of satellite failures in large constellations, the impact of failed satellite numbers on the coverage performance of constellation was analyzed[19].

（1） Comparison of the position distribution of failed satellites

The simulation scenarios in this section are as follows:

i. No satellite failures;
ii. 20% satellite failures concentrated in adjacent orbits;
iii. 20% of the satellites fail and are randomly distributed within the same orbital layer;
iv. 20% of the satellites fail and are randomly distributed in two orbital layers.

Firstly, the variations in coverage performance under the first three scenarios were analyzed, as shown in Firstly, the variations in coverage performance under the first three scenarios were analyzed, as shown in Fig. 9. It can be observed that the location of failed satellites has a significant impact on coverage duration and revisit time. When failed satellites are concentrated in adjacent orbits, the average coverage duration decreases by 2432 seconds, while the average revisiting time increases by 335 seconds. At 4°N latitude, the coverage performance experiences the largest change, with a reduction of 8.7% in coverage duration and an increase of 2128 seconds in revisit time. In contrast, the change in coverage multiplicity is relatively small, with an average decrease of 0.07. It is evident that when failed satellites are distributed in a concentrated manner, the coverage performance in some regions can be significantly degraded. As shown in Fig. 9, when failed satellites are randomly distributed, the coverage performance remains almost unchanged.

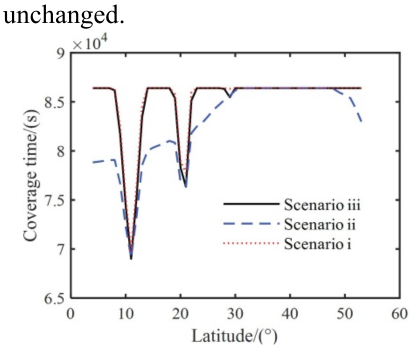

(a) Coverage time performance

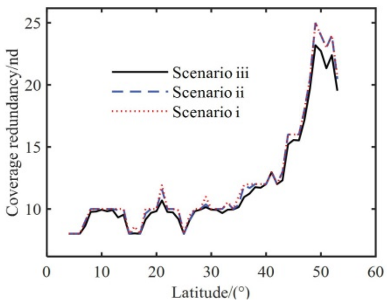

(b) Coverage redundancy performance

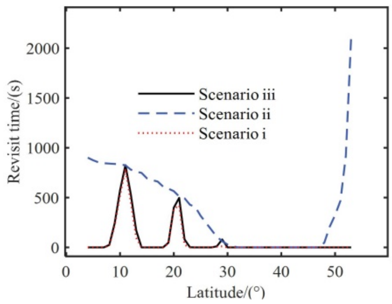

(c) Revisit time performance

Figure 9 Comparison of coverage performance with different failure satellite distributions

To further quantify the impact of the location distributions of failed satellites on the constellation, the coverage performance values under scenario iii and iv were compared with those under scenario i, as shown in Fig. 10. Although each indicator has a different degree of decrease, the decrease is still very small. After variance analysis, the significance levels of the three indicators were far greater than 0.01. Therefore, it can be concluded that under the simulation scenarios of this paper, if the positions of the failed satellites are randomly distributed, the coverage performance of the constellation will not experience significant changes.

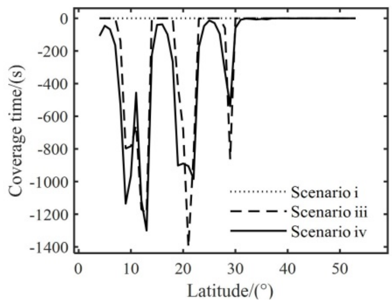

(a) Coverage time performance

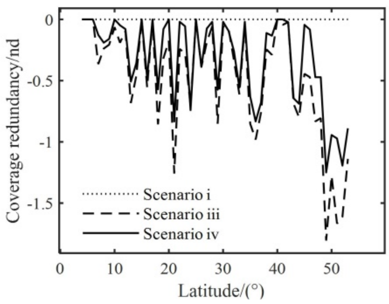

(b) Coverage redundancy performance

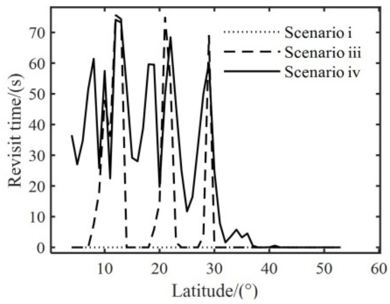

(c) Revisit time performance

Figure 10 Comparison of coverage performance with randomly distributed failed satellites at different layers

（2） Comparison of the number of failed satellites

Considering that 20% of the satellites in the constellation have already failed, the debris density is likely to have reached the critical value of Kessler syndrome, causing the number of debris to increase like a snowball, leading to more satellite failures. Therefore, this paper introduces two new scenarios:

v. 30% satellite failures with random distribution in the same orbital layer;
vi. 40% satellite failures with random distribution in the same orbital layer.

As shown in Fig 11, the average number of impacts per satellite in the constellation is 43 and 58. Although the number of failed satellites varies, the trend of coverage performance with latitude remains generally consistent. Compared to the scenario iii, in scenario v, the coverage duration decreases by 0.5%, the coverage redundancy decreases by 2.1%, and the revisiting time increases by 42.8 seconds; in scenario vi, the coverage duration decreases by 1.3%, the coverage redundancy decreases by 5.8%, and the revisiting time increases by 90.5 seconds. The variation in coverage indicators under the three scenarios is relatively small, as even with 40% of satellites failing, there are still 1,900 operative satellites in the constellation, which can maintain the operation of constellation. However, as the number of failed satellites increases, the decline in coverage performance will become more significant, accompanied by the Kessler effect "infecting" the remaining satellites like an infectious disease, affecting the entire constellation.

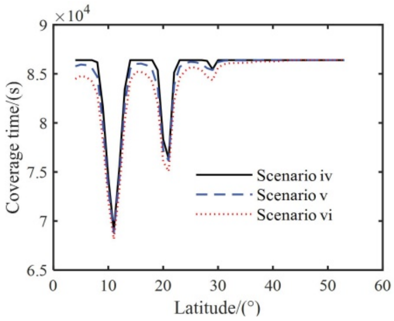

(a) Coverage time performance

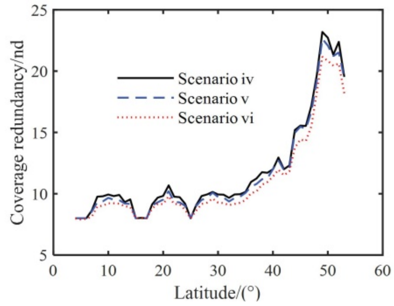

(b) Coverage redundancy performance

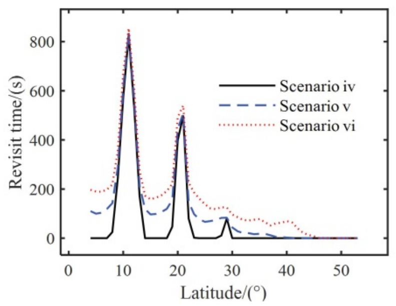

(c) Revisit time performance

Figure 11 Comparison of constellation coverage performance with different numbers of failed satellites

（3） Comprehensive comparison

Fig. 12shows the variation of constellation coverage performance with latitude in different scenarios, where the coverage capability is derived from the weighted sum of three indicators using the entropy weight method, and the constellation status represents different scenarios. When the failed satellites are concentrated in certain areas, the coverage capability in those regions can significantly decrease, even falling below 40% of the coverage capability when 40% of the satellites fail. However, when 20% of the failed satellites are randomly distributed, the performance change is minimal. Yet, as the number of failed satellites increases to 30% or even 40%, the coverage capability will also significantly decrease.

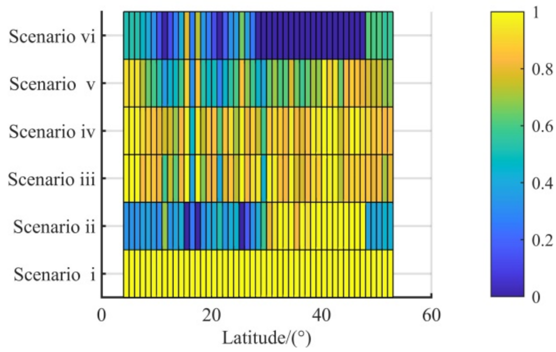

Figure 12 Comparison of coverage performance after weighting under different scenarios

4 CONCLUSION

In this paper, a satellite risk assessment algorithm based on shielding algorithm and Monte Carlo impact simulation method is proposed for satellite risk assessment in uncertain space debris environment, and the correspondence between the number of impacts and the failure probability is obtained. Furthermore, the perspective is elevated from the satellite to the constellation, combining the failure probability of single satellite, the number of impacts, and the coverage performance of the constellation. The entropy weighting method is used to balance the weights of different evaluation indicators, analyzing the impacts of the number of failed satellites and their locations on the constellation coverage performance, and arriving at the following conclusions:

- If the locations of failed satellites are centrally distributed, the coverage performance of some areas will be greatly reduced;
- If the locations of failed satellites are randomly distributed, the change in coverage performance is minimal;
- As the number of failed satellites increases, the rate of decline in coverage performance accelerates.

The method proposed in this paper connects space debris with complex constellation systems, analyzing the impact of debris uncertainty on satellites and constellations. It achieves a certain degree of quantitative assessment of satellite risk and constellation system performance, providing reference for spacecraft protection design and the subsequent construction and optimization of large constellation systems.

ACKOWLEDGMENTS

This work was supported by the Shanghai Aerospace Science and Technology Innovation Funds (SAST2022-022 and SAST2022-113).

REFERENCES

1. McDowell, J. (2024). Space activities in 2023. Online at *http:// planet4589.org/space/papers/space22.pdf.*

2. Christiansen, E. (2014). MMOD protection and degradation effects for thermal control systems.Online at *https://ntrs.nasa.gov/archive/nasa/casi.ntrs.nasa.gov/20140010668.pdf.*

3. Palmer, C. (2022). Russian anti-satellite test spotlights space debris danger. *Engineering*. 12(3), 3–5.

4. Christiansen, E. L., Nagy, S., et al. (2016). Bumper 3 update for IADC protection manual. Online at *https://ntrs.nasa.gov/archive/nasa/casi.ntrs.nasa.gov/20160003137.pdf.*

5. Ruhl, K., Bunte, K. D., Gaede, A., et al. (2014). ESABASE2-Debris software user manual. Online at *https://esabase2.net/wp-content/uploads/2015/12/esabase2-debris-user-manual.pdf.*

6. Hu, D., Pang, B., Chi, R., et al. (2021). Survivability assessment of spacecraft impacted by orbit debris. *Defence Technology*. 17(3), 961-970.

7. Chi, R., Liu, Y., Hu, D., et al. (2024). An impact sensitivity assessment method of spacecraft based on virtual exterior wall. *Defence Technology*. 31(1), 142-157.

8. Olivieri, L., & Francesconi, A. (2020). Large constellations assessment and optimization in LEO space debris environment. *Advances in Space Research*. 65(1), 351-363.

9. Wilmer, A. P., Boone, N. R., & Bettinger, R. A. (2022). Debris propagation and spacecraft survivability assessment for catastrophic mishaps occurring in cislunar periodic orbits. *Journal of Space Safety Engineering*. 9(2), 207-222.

10. Trisolini, M., Lewis, H. G., & Colombo, C. (2018). Spacecraft design optimisation for demise and survivability. *Aerospace Science and Technology*. 77, 638–657.

11. Carmen, P., & Luciano, A. (2023). The short-term effects of the Cosmos 1408 debrisation on neighboring inhabited space stations and large constellations. *Acta Astronautica*. 210, 465-473.

12. Maria, E. P., Luis, J. G., & Camilla, C. (2023). Analytical model for impact probability assessments with large satellite constellations. *Advances in Space Research*. 72(7), 2515-2534.

13. Tao, H., Che, X., Zhu, Q., & Li, X. (2022). Satellite in-orbit secondary collision risk assessment. *International Journal of Aerospace Engineering*. 2022(1), 6358188.

14. Yuan, Y., Yang, K., Zhang, J., et al. (2024). Impact of constellation satellite explosions on the space debris environment evolution. *Journal of Astronautics*. 45(5), 790-798.

15. Sun, J., Zhang, G., & Liu, Z. (2023). Constellation coverage performance analysis based on Markov-ADC model. *Chinese Journal of Space Science and Technology*. 43(5), 24-34.

16. Xue, W., Hu, M., Ruan, Y., & Wang, X. (2023). Analysis performance of navigation constellation satellite failure and enhancement of LEO navigation. *Journal of Physics: Conference Series*. 2551(1), 012012.

17. IADC WG3 members. (2011). Protection manual (IADC-04-03). Online at *https://iadc-home.org/documents_public/view/id/81#u.*

18. Zheng, J.,Zhou, J.,Pi, X, et al. (2021). Hypervelocity impact on volt-ampere characteristic of solar arrays by using two-stage light gas gun. *Acta Physica Sinica*. 70(18).

19. Boley, A. C., & Byers, M. (2021). Satellite mega-constellations create risks in low Earth orbit, the atmosphere, and on Earth. *Scientific Reports*. 11(1), 1-8.

20. Li, H., Li, D., & Li, Y. (2018). A multi-index assessment method for evaluating coverage effectiveness of remote sensing satellite. *Chinese Journal of Aeronautics*. 31(10), 2023-2033.